Appl Phys B (2012) 107:131–136
DOI 10.1007/s00340-011-4853-0

Applied Physics B
Lasers and Optics

Femtosecond energy relaxation in suspended graphene: phonon-assisted spreading of quasiparticle distribution

J. Shang · T. Yu · G.G. Gurzadyan

Received: 6 September 2011 / Revised version: 24 October 2011 / Published online: 14 January 2012

Abstract Ultra-fast optical measurements of few-layer suspended graphene films grown by chemical vapor deposition were performed with femtosecond pump–probe spectroscopy. The relaxation processes were monitored in transient differential transmission ($\Delta T/T$) after excitation at two different wavelengths of 350 and 680 nm. Intraband electron–electron scattering, electron–phonon scattering, interband Auger recombination and impact ionization were considered to contribute to $\Delta T/T$. All these processes may play important roles in spreading the quasiparticle distribution in time scales up to 100 fs. Optical phonon emission and absorption by highly excited non-equilibrium electrons were identified from $\Delta T/T$ peaks in the wide spectral range. When the probe energy region was far from the pump energy, the energy dependence of the quasiparticle decay rate was found to be linear. Longer lifetimes were observed when the quasiparticle population was localized due to optical phonon emission or absorption.

1 Introduction

Graphene, a monolayer of carbon atoms, provides an excellent platform to investigate the quasiparticle dynamics in the two-dimensional material [1]. The dynamics is strongly related to the unique electronic structure of graphene, especially the linear energy dispersion spectrum around the Dirac point, which has attracted considerable efforts to interpret in theory and experiment [1–4]. It is very important to study the quasiparticle dynamics for fundamental quantum mechanics and graphene-based electronic and optical devices, such as field-effect transistors [5] and saturable absorbers for ultra-fast pulsed lasers [6]. Experimentally, ultra-fast spectroscopy is a direct approach for observation of dynamic scattering events among quasiparticles using ultra-short pulses. Femtosecond pump–probe measurements [7–16] of various graphene films have been reported, where time scales of relaxation processes of excited electrons range from femtoseconds to tens of picoseconds. Recently, electron–electron (e-e) and electron–optical phonon (e-op) scattering processes were also investigated by photoluminescence measurements [17–19] of graphene under ultra-fast laser excitation, where both contribute to the broad emission spectra [17].

It is noted that, in previous studies [7–19], most graphene films are epitaxial graphene films on SiC substrates [7–9] or exfoliated layers from graphite [13, 16–19]. In contrast to the promising applications [3, 6] of large-area graphene films grown by chemical vapor deposition (CVD), their ultra-fast properties have not caused enough attention [10, 15]. Further, due to the influence of the substrate on the electronic structure [20, 21] and the electron dynamics [22] of graphene, the suspended sample is expected to reflect more intrinsic properties of graphene itself compared to the supported graphene films, where the scattering of electrons can be related to extrinsic sources such as remote interfacial phonons [23, 24]. On the other hand, there is a quite attractive topic about the dynamic quasiparticle distribution after photon excitation. It can offer more complete information of the relaxation progression of excited electrons in

J. Shang · T. Yu · G.G. Gurzadyan (✉)
Division of Physics and Applied Physics, School of Physical and Mathematical Sciences, Nanyang Technological University, Singapore 637371, Singapore
e-mail: gurzadyan@ntu.edu.sg

T. Yu
Department of Physics, Faculty of Science, National University of Singapore, Singapore 117542, Singapore
e-mail: yuting@ntu.edu.sg

the electronic band than that of the relaxation dynamics at a probed energy level. However, only a few studies were reported on this topic of graphene [8, 10, 16]. Our previous studies have focused on ultra-fast relaxation processes of monolayer, bilayer and stacked CVD-grown graphene films [10–12] by a UV/visible pump–probe setup, where quasiparticle lifetimes and their energy dependences were reported. In this paper, quasiparticle dynamics of suspended CVD-grown few-layer graphene has been studied by using two different pump wavelengths, 350 and 680 nm, and using the probe beam in the visible (400–650 nm). For the first time we observe both ultra-fast optical phonon emission and absorption in transient differential transmission ($\Delta T/T$) spectra of the few-layer graphene.

2 Experimental

The few-layer graphene sample was grown on high-purity (99.999%) copper foil by low-pressure thermal CVD, where the growth mechanism is a surface-catalyzed and self-limiting process involved with the low solubility of carbon in copper [12, 25]. The obtained few-layer graphene on copper was put in an aqueous solution of iron nitride, $(FeNO_3)_3$, for etching the copper foil. Finally, the floating few-layer graphene was transferred onto a silicon substrate with pre-patterned holes of 270 μm in diameter. The ultra-fast optical measurements were conducted by focusing the laser beam on the suspended parts. Surface images were taken by a scanning electron microscope (SEM, JEOL JSM-6700F) where the operating voltage was set at 10 kV. A Raman system (WITec CRM 200) with a diode-pumped double-frequency Nd:YAG laser (532 nm) was employed to acquire Raman spectra. The steady state transmission spectrum was determined by an UV–Vis spectrophotometer (Cary 100Bio, Varian) in the spectral range from 400 to 800 nm. For pump–probe measurements, the 800-nm output of a titanium–sapphire regenerative amplifier (Legend Elite, Coherent) seeded by an oscillator (Micra, Coherent) was used as a pulse laser source: pulse width 80 fs, pulse repetition rate 1 kHz and average power 2.6 W. 90% of the radiation was converted into the pump beam of 350 nm or 680 nm by passing an optical parametric oscillator. The remaining 10% was used to obtain the probe beam of white-light continuum. The details of this pump–probe system have been described in a previous work [11]. The kinetic data were fitted to a multi-exponential decay function convoluted with the instrument response function. The full widths at half maximum (FWHMs) of the instrument response functions were about 120 fs and 90 fs at the excitation wavelengths of 350 and 680 nm, respectively.

3 Results and discussion

Figures 1a–1c show SEM images of the suspended graphene sample with magnifications of 250, 2000 and 10000, respectively. It is clear that the graphene film is suspended over a hole with a diameter of 270 μm. There are some ripple and/or fold structures found on the surface of the sample. The transmission spectrum of the few-layer graphene on quartz is shown in Fig. 1d and proves that the opacity of the sample is close to a few times the value of monolayer graphene (2.3%) [26], which is similar to those transmission spectra of few-layer graphene films in other studies [27]. To further confirm the number of graphene layers, Raman spectra of suspended monolayer, bilayer, few-layer CVD-grown graphene and graphite were recorded as shown in Figs. 1e and 1f. G-band positions for all samples are similar at 1580 ± 2 cm^{-1}. The position and the FWHM of 2D bands increase with the number of graphene layers. By discriminating the Raman characteristics of graphene films and graphite, i.e. the FWHM (54 ± 4 cm^{-1}) and the position (2700 ± 2 cm^{-1}) of 2D bands, the suspended sample used here is identified to be a few-layer graphene film, which is in

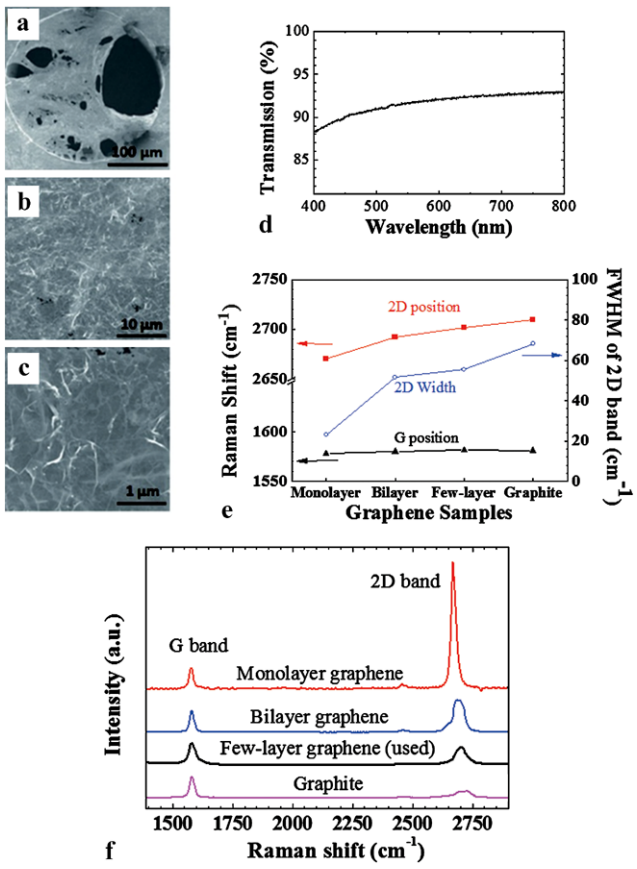

Fig. 1 SEM images (**a**–**c**) of the suspended few-layer graphene film, the transmission spectrum (**d**) of the transferred few-layer graphene on quartz and Raman spectra (**e**, **f**) of the suspended few-layer graphene film

agreement with previous reports [28, 29]. G and 2D bands in graphene and graphite films are associated with two species of phonons, zone-center and zone-boundary optical phonons at Γ and K in the phonon dispersion curve [30], respectively. For the few-layer graphene, the zone-center and the zone-boundary phonon energies are estimated to be 0.196 (for G band) and 0.168 eV (for D band), respectively.

Figures 2a and 2b show transient differential transmission spectra of the suspended graphene for two excitation energies, 3.55 and 1.83 eV, respectively. In the investigated energy range, the conduction and valence bands are almost symmetric [31] referring to the momentum axis in the schematic electronic band as shown in the insets of Fig. 2 (k-axis). According to previous studies [4, 32, 33], $E - E_{\mathrm{f}}$ is used to represent the excited and detected energy levels, which are equal to half of the pump and probe photon energies [7, 13, 15, 16, 18, 32, 33], respectively. E_{f} (0 eV) is the Fermi energy and located at the touching region of conduction and valence bands [31]. The positive $\Delta T/T$ indicates induced transmission or bleaching by the pump pulse, which conveys the information on the quasiparticle distribution in the electronic band of few-layer graphene. The real-time evolution of this distribution reveals the relaxation progression of all excited electrons in the probed electronic band. In Fig. 2a, the intensity of $\Delta T/T$ decreases with the pump–probe delay, and two series of discrete peaks at 1.2 ± 0.03 and 1.35 ± 0.03 eV (denoted by dotted arrows) were discerned. The energy intervals between these two groups of peaks are about 0.15 eV, which corresponds to the energy of a zone-boundary optical phonon (derived from the Raman data above). These peaks can be assigned to enhanced transmission by the third- and the fourth-order optical phonon emissions starting from the laser-excited level 1.78 eV, which is half of the pump photon energy, due to the symmetric electronic structure [2, 3]. Analogous features in GaAs [34] and GaN/AlGaN heterostructure [35] were also observed by femtosecond transmission spectroscopy, which resulted from longitudinal optical phonon emission. In detail, the peak positions slightly shift towards high energies with the delay time. We explain this shift as the result of the increase of the lattice temperature due to the energy transferred from the electron to the lattice, which can shorten the optical phonon energy, in accordance with Raman studies of 2D-band red shift versus temperature in graphene [36, 37]. It should be mentioned that the first- and the second-order peaks caused by optical phonon emission (Fig. 2a) are not observable because of the weak probe light at $\lambda < 400$ nm and the bad signal-to-noise ratio.

Except for the peak regions, i.e. phonon replicas, the background of $\Delta T/T$ in Fig. 2a corresponds to the occupied states in the probed energy levels that are caused by the downward spreading of the excited electrons after photoexcitation. The decrease of the intensity of the background

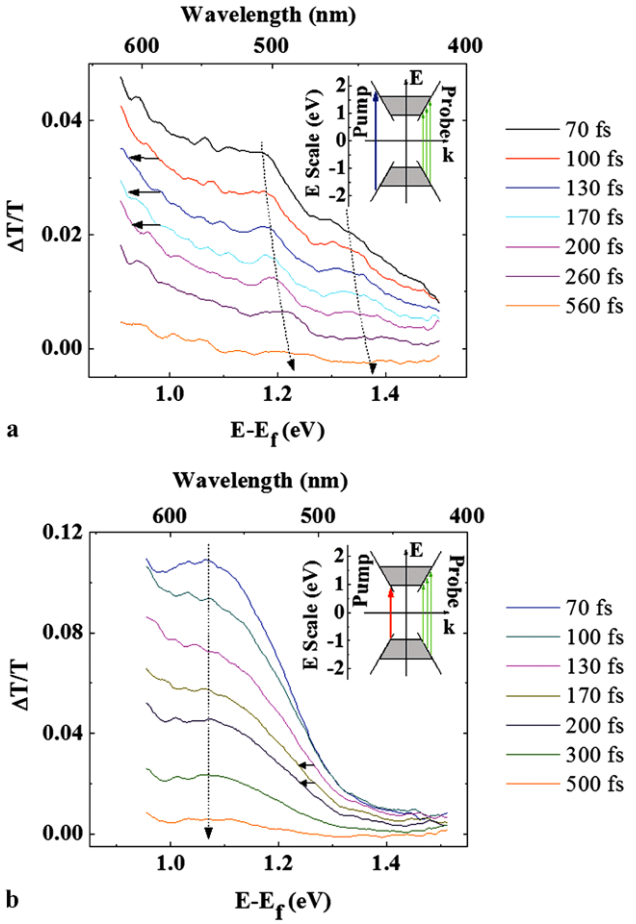

Fig. 2 Transient $\Delta T/T$ spectra of the suspended few-layer graphene film at the excitation energies of (**a**) 3.55 eV (350 nm) and (**b**) 1.83 eV (680 nm). *Insets*: schematics of the electronic band structure of the few-layer graphene film and pump/probe transitions

indicates that the excited electrons relax to the lower energy levels. Similar behavior has also been observed in the monolayer and stacked graphene films [11, 16]. In order to estimate quantitatively the red shift of the transient spectra with time, the typical energy relaxation rates were calculated by comparing the energies ($E - E_{\mathrm{f}}$) of adjacent transient spectra at the same $\Delta T/T$ intensity (as shown by the black solid arrows in Fig. 2a). For example, in the energy region around $E - E_{\mathrm{f}} = 0.95$ eV, the transient spectra at 100, 130, 170 and 200 fs were selected to get the average energy relaxation rate: 1.6 ± 0.2 meV/fs. According to a recent report on reduced graphene oxide films [38], the optical phonon emission time is extracted by dividing the phonon energy by the relaxation rate, i.e. in our case 0.15 eV/(1.6 meV/fs) = 90 fs, where 0.15 eV is the detected phonon energy. Note that our obtained result (1.6 meV/fs) in the few-layer graphene sample is smaller than the one (4–10 meV/fs) of reduced graphene oxide films [38].

However, for optical phonon absorption (Fig. 2b) we did observe the broad first-order peak centered at $1.07 \pm$

0.02 eV, which is about 0.15 eV away from the laser-excited energy of 0.92 eV. The background of the $\Delta T/T$ spectrum represents the induced transmission due to only upward spreading of excited electrons. The energy relaxation rate can be calculated by the energy shift of the $\Delta T/T$ spectrum towards low energies. For instance, at energies of about $E - E_f = 1.25$ eV and times of 130, 170 and 200 fs (indicated by black solid arrows, Fig. 2b), the obtained relaxation rate and the optical phonon emission time are 0.9 ± 0.1 meV/fs and ~170 fs, respectively. After 100 fs, i.e. when the e-e scattering contribution is low, the $\Delta T/T$ spectrum reflects a combinational effect of two processes: optical phonon emission and absorption. These two processes are related to the decrease and the increase of the total energy of the excited electron system, respectively. Decay of the $\Delta T/T$ signal at 1.08 eV originates from the reduction of total energy of the excited electron system, which means that optical phonon emission overcomes optical phonon absorption during e-op scattering. In comparison with the zone-boundary optical phonon, emission or absorption of the zone-center optical phonon (0.196 eV) has not been observed in Fig. 2. Thus, the obtained results evidence the previous theoretical predictions that the e-op scattering at K is prevailing rather than e-op scattering occurring equally likely at both Γ and K [39, 40]; it is consistent with the phonon-related fluctuations (~0.15 eV) obtained from angle-resolved photon emission spectroscopy [41] and scanning tunneling microscopy [42, 43].

Figure 3 presents the kinetic curves of $\Delta T/T$ and the energy dependences of quasiparticle decay rates after excitation with 3.55 eV (350 nm) and 1.83 eV (680 nm). The decay curves for the energies at 1.0 and 1.2 eV can well be

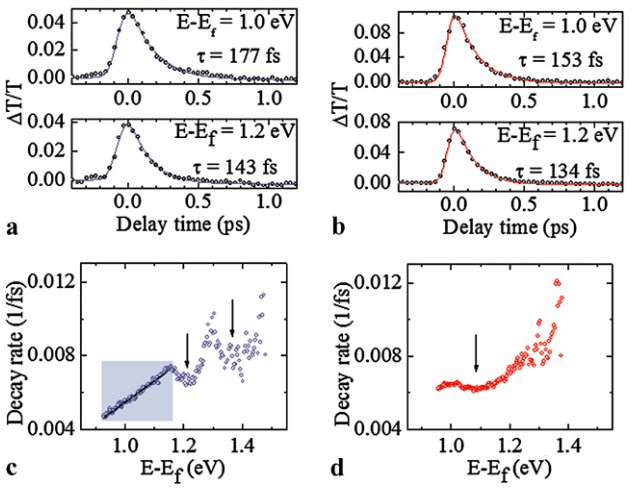

Fig. 3 (**a**, **b**) Kinetic behavior of $\Delta T/T$ as a function of pump–probe delay for the suspended few-layer graphene film pumped at 3.55 eV (350 nm) and 1.83 eV (680 nm), respectively. (**c**, **d**) Quasiparticle decay rates versus quasiparticle energy at the excitation energies of 3.55 eV and 1.83 eV, respectively

fitted by a mono-exponential function. The decay process is appointed to the e-op scattering as reported in Refs. [9] and [10]. As shown in Fig. 3c and 3d, the quasiparticle lifetimes range from 90 to 220 fs at the probed energy levels. A linear relationship with a slope of 0.012 ± 0.01 eV^{-1} fs^{-1} was observed in the energy range from 0.9 to 1.15 eV at 350-nm excitation (Fig. 3c), which reflects the linear density of states, as expected from previous studies [44–46]. It was noted that this linear region is far (>0.6 eV) from the laser-excited level. Moreover, two obvious valleys were found at about 1.21 and 1.37 eV, where the quasiparticle decay rates drop down. It is found that the positions of these valleys coincide with the peak locations in the transient $\Delta T/T$ spectra in Fig. 2a, where the quasiparticle population in the peak region is relatively higher than those in non-peak regions referring to the background. Therefore, the anomalous behavior (valleys) in Fig. 3c is attributed to the extra quasiparticle accumulation in these regions, i.e. localization of the quasiparticle population, induced by the third- and the fourth-order optical phonon emissions as discussed above (Fig. 2a). Meanwhile, when the sample was pumped at 680 nm, one concave region was recognized to be located around 1.08 eV, corresponding to the first-order optical phonon absorption (Fig. 3d). After this turning region, the quasiparticle decay rate increases versus the energy of $E - E_f$ (E_f is the Fermi energy).

By combining the transient $\Delta T/T$ spectra and kinetics data, a more detailed understanding of early quasiparticle relaxation processes is obtained. In the first 50 fs, the electron population spreads upward and downward from the laser-excited level. In general, if the relaxation of electrons is caused only by the electron–phonon scattering, the transient spectrum is expected to show the periodic peaks without the strong background [47]. However, the large background is observed in the first 100 fs (Fig. 2), indicating the existence of other relaxation channels besides electron–phonon scattering. We consider three processes which lead to ultrafast spreading of the quasiparticle population: intraband e-e scattering, interband Auger processes and electron–phonon scattering. First, intraband elastic and inelastic e-e scattering events can result in the randomization of momentum and energy followed by Coulomb thermalization causing the formation of a Fermi–Dirac distribution of quasiparticles, similar to semiconductors, e.g. GaAs and Ge [48]. The e-e scattering time in graphene has been estimated based on Z-scan [49] and two-pulse correlation measurements [17], where the typical time scale is around 10 fs. Therefore, intraband e-e scattering does contribute to the quasiparticle spreading. Recently, the possibility of Auger processes induced by the excited electrons and their influence on carrier dynamics in graphene materials have been theoretically studied by Winzer et al. [50]. For interband Auger processes, Auger recombination may arouse the upward spreading of

the electron distribution referring to the laser-excited level and impact ionization can cause the downward spreading, where the excited electron is losing energy [15, 50]. Particularly, both Auger processes can take place at the early times (<50 fs) after photo-excitation [50]. Therefore, Auger processes may serve for the observed large background. Similarly, recent experimental reports [15, 16] also pointed out the role of Auger processes in the early times of photo-excited mono- and multilayer graphene films. Within 100 fs, a considerable number of phonons are created, which further participate in the energy relaxation of electrons. In our case, ultra-fast phonon emission and absorption play a distinct role in the early spreading of quasiparticles which cause the formation of transient phonon replicas in the $\Delta T/T$ spectra. Strong optical phonon emission or absorption will affect the populations and the lifetimes of quasiparticles at energies close to the laser-excited level, i.e. 1.36 and 1.07 eV. After 100 fs, optical phonon emission is predominant rather than optical phonon absorption, and the energy relaxation is regulated by the e-op scattering in the probed energy range. As a result, the total quasiparticle distribution shifts to low energies.

4 Conclusions

In conclusion, quasiparticle dynamics of suspended few-layer graphene films grown by CVD has been studied by use of femtosecond spectroscopy techniques. The phonon emitted or absorbed during the broadening of the electron distribution was recognized as a zone-boundary optical phonon with the energy of 0.15 ± 0.02 eV. Linear dependence of the quasiparticle decay rate on electron energy was observed in the energy levels far (>0.6 eV) from the laser-excited level of 1.78 eV. Localization of the quasiparticle population induced by the first-order optical phonon absorption and the higher order (third and fourth) optical phonon emissions was distinguished, where the kinetic curve behaved with a slow decay.

Acknowledgements We are grateful to Prof. Maria-Elisabeth Michel-Beyerle for continuous support and Prof. Jianyi Lin for providing the CVD system. J. Shang thanks Dr. Zhiqiang Luo, Dr. Xiaofeng Fun and Mr. Jiaxu Yan for discussing the results. T. Yu thanks the support of the Singapore National Research Foundation under NRF Award No. NRF-RF2010-07 and MOE Tier 2 MOE2009-T2-1-037.

References

1. A. Bostwick, T. Ohta, T. Seyller, K. Horn, E. Rotenberg, Nat. Phys. **3**, 36 (2007)
2. A.H. Castro Neto, F. Guinea, N.M.R. Peres, K.S. Novoselov, A.K. Geim, Rev. Mod. Phys. **81**, 109 (2009)
3. Y.H. Wu, T. Yu, Z.X. Shen, J. Appl. Phys. **108**, 071301 (2010)
4. M. Sprinkle, D. Siegel, Y. Hu, J. Hicks, A. Tejeda, A. Taleb-Ibrahimi, P. Le Fèvre, F. Bertran, S. Vizzini, H. Enriquez, S. Chiang, P. Soukiassian, C. Berger, W.A. de Heer, A. Lanzara, E.H. Conrad, Phys. Rev. Lett. **103**, 226803 (2009)
5. K.S. Novoselov, A.K. Geim, S.V. Morozov, D. Jiang, Y. Zhang, S.V. Dubonos, I.V. Grigorieva, A.A. Firsov, Science **306**, 666 (2004)
6. Q. Bao, H. Zhang, Y. Wang, Z. Ni, Y. Yan, Z.X. Shen, K.P. Loh, D.Y. Tang, Adv. Funct. Mater. **19**, 1 (2009)
7. J.M. Dawlaty, S. Shivaraman, M. Chandrasekhar, F. Rana, M.G. Spencer, Appl. Phys. Lett. **92**, 042116 (2008)
8. D. Sun, Z.-K. Wu, C. Divin, X.B. Li, C. Berger, W.A. de Heer, P.N. First, T.B. Norris, Phys. Rev. Lett. **101**, 157402 (2008)
9. L. Huang, G.V. Hartland, L.Q. Chu, Luxmi, R.M. Feenstra, C. Lian, K. Tahy, H. Xing, Nano Lett. **10**, 1308 (2010)
10. J. Shang, Z. Luo, C. Cong, J. Lin, T. Yu, G.G. Gurzadyan, Appl. Phys. Lett. **97**, 163103 (2010)
11. J. Shang, T. Yu, J. Lin, G.G. Gurzadyan, ACS Nano **5**, 3278 (2011)
12. Z. Luo, T. Yu, J. Shang, Y. Wang, S. Lim, L. Liu, G.G. Gurzadyan, Z. Shen, J. Lin, Adv. Funct. Mater. **21**, 911 (2011)
13. R.W. Newson, J. Dean, B. Schmidt, H.M. van Driel, Opt. Express **17**, 2326 (2009)
14. F. Carbone, G. Aubock, A. Cannizzo, F. Van Mourik, R.R. Nair, A.K. Geim, K.S. Novoselov, M. Chergui, Chem. Phys. Lett. **504**, 37 (2011)
15. P.A. Obraztsov, M.G. Rybin, A.V. Tyurnina, S.V. Garnov, E.D. Obraztsova, A.N. Obraztsov, Y.P. Svirko, Nano Lett. **11**, 1540 (2011)
16. M. Breusing, S. Kuehn, T. Winzer, E. Malíc, F. Milde, N. Severin, J.P. Rabe, C. Ropers, A. Knorr, T. Elsaesser, Phys. Rev. B **83**, 153410 (2011)
17. C.H. Lui, K.F. Mak, J. Shan, T.F. Heinz, Phys. Rev. Lett. **105**, 127404 (2010)
18. W.-T. Liu, S.W. Wu, P.J. Schuck, M. Salmeron, Y.R. Shen, F. Wang, Phys. Rev. B **82**, 081408 (2010)
19. R.J. Stöhr, R. Kolesov, J. Pflaum, J. Wrachtrup, Phys. Rev. B **82**, 121408 (2010)
20. F. Varchon, R. Feng, J. Hass, X. Li, B. Ngoc Nguyen, C. Naud, P. Mallet, J.-Y. Veuillen, C. Berger, E.H. Conrad, L. Magaud, Phys. Rev. Lett. **99**, 126805 (2007)
21. S.Y. Zhou, G.-H. Gweon, A.V. Fedorov, P.N. First, W.A. de Heer, D.-H. Lee, F. Guinea, A.H. Castro Neto, A. Lanzara, Nat. Mater. **6**, 770 (2007)
22. S. Fratini, F. Guinea, Phys. Rev. B **77**, 195415 (2008)
23. X. Du, I. Skachko, A. Barker, E.Y. Andrei, Nat. Nanotechnol. **3**, 491 (2008)
24. J.H. Chen, C. Jang, S. Xiao, M. Ishigami, M.S. Fuhrer, Nat. Nanotechnol. **3**, 206 (2008)
25. X. Li, W. Cai, L. Colombo, R.S. Ruoff, Nano Lett. **9**, 4268 (2009)
26. R.R. Nair, P. Blake, A.N. Grigorenko, K.S. Novoselov, T.J. Booth, T. Stauber, N.M.R. Peres, A.K. Geim, Science **320**, 1308 (2008)
27. K.S. Kim, Y. Zhao, H. Jang, S.Y. Lee, J.M. Kim, K.S. Kim, J.-H. Ahn, P. Kim, J.-Y. Choi, B.H. Hong, Nature **457**, 706 (2009)
28. Z. Ni, Y. Wang, T. Yu, Z. Shen, Nano Res. **1**, 273 (2008)
29. Y. Hao, Y. Wang, L. Wang, Z. Ni, Z. Wang, R. Wang, C.K. Koo, Z. Shen, J.T.L. Thong, Small **6**, 195 (2010)
30. L.M. Malard, M.A. Pimenta, G. Dresselhaus, M.S. Dresselhaus, Phys. Rep. **473**, 51 (2009)
31. B. Partoens, F.M. Peeters, Phys. Rev. B **74**, 075404 (2006)
32. G. Moos, C. Gah, R. Fasel, M. Wolf, T. Hertel, Phys. Rev. Lett. **87**, 2674021 (2001)
33. C.D. Spataru, M.A. Cazalilla, A. Rubio, L.X. Benedict, P.M. Echenique, S.G. Louie, Phys. Rev. Lett. **87**, 2464051 (2001)
34. C. Fürst, A. Leitenstorfer, A. Laubereau, R. Zimmermann, Phys. Rev. Lett. **78**, 3733 (1997)

35. Z. Wang, K. Reimann, M. Woerner, T. Elsaesser, D. Hofstetter, J. Hwang, W.J. Schaff, L.F. Eastman, Phys. Rev. Lett. **94**, 037403 (2005)
36. I. Calizo, S. Ghosh, W. Bao, F. Miao, C.N. Lau, A.A. Balandin, Solid State Commun. **149**, 1132 (2009)
37. D.J. Late, U. Maitra, L.S. Panchakarla, U.V. Waghmare, C.N.R. Rao, J. Phys., Condens. Matter **23**, 055303 (2011)
38. B.A. Ruzicka, N. Kumar, S. Wang, K.P. Loh, H. Zhao, J. Appl. Phys. **109**, 084322 (2011)
39. N. Bonini, M. Lazzeri, N. Marzari, F. Mauri, Phys. Rev. Lett. **99**, 176802 (2007)
40. H. Suzuura, T. Ando, Inst. Phys. Conf. Ser. **150**, 022080 (2009)
41. S.Y. Zhou, D.A. Siegel, A.V. Fedorov, A. Lanzara, Phys. Rev. B **78**, 193404 (2008)
42. G. Li, A. Luican, E.Y. Andrei, Phys. Rev. Lett. **102**, 176804 (2009)
43. V.W. Brar, S. Wickenburg, M. Panlasigui, C.-H. Park, T.O. Wehling, Y. Zhang, R. Decker, C. Girit, A.V. Balatsky, S.G. Louie, A. Zettl, M.F. Crommie, Phys. Rev. Lett. **104**, 036805 (2010)
44. J. Gonzalez, E. Perfetto, Phys. Rev. Lett. **101**, 176802 (2008)
45. B. Partoens, F.M. Peeters, Phys. Rev. B **74**, 075404 (2006)
46. V.N. Kotov, B. Uchoa, V.M. Pereira, A.H. Castro Neto, F. Guinea, arXiv:1012.3484v1 (2010)
47. F. Rossi, T. Kuhn, Rev. Mod. Phys. **74**, 895 (2002)
48. A. Othonos, J. Appl. Phys. **83**, 1789 (1998)
49. G. Xing, H. Guo, X. Zhang, T.C. Sum, C.H.A. Huan, Opt. Express **18**, 4564 (2010)
50. T. Winzer, A. Knorr, E. Malic, Nano Lett. **10**, 4839 (2010)